Study of Neutron Resonances by Low Energy Neutron Tagging (LENT)

Submitted by

K. Assamagan, O.K. Baker, C.E. Keppel (spokesperson), I. Niculescu
L. Tang

Hampton University

R. Ent (spokesperson), H.C. Fenker, A. Lung, D. Mack
J.H. Mitchell (spokesperson), W.F. Vulcan, S.A. Wood

Jefferson Laboratory

J.R. Calarco

University of New Hampshire

Abstract

We propose to measure neutron resonance electroproduction spectra in the intermediate Q^2 range $1 < Q^2 < 4$ $(\text{GeV/c})^2$ and to measure F_2^{en} at $x = 0.65$ and $Q^2 = 5$. For these measurements, a tagged neutron detector facility is proposed. The facility will consist of a neutron tagging detector to measure low energy recoiling protons originating in a 1 cm diameter 4 cm long deuterium target. Such a facility could serve as a general purpose tool for the study of neutron structure.

MOTIVATION

While precision electron-proton scattering experiments have been accomplished in a straightforward manner with hydrogen targets, it has been necessary to infer experimental information on the structure of the neutron from nuclear (typically deuteron) data. The procedure of unfolding neutron data from inclusive nuclear cross sections, via the subtraction of Fermi motion effects and contributions from various nuclear constituents, leads to ambiguities dependent on the models and reaction mechanisms employed. This is particularly true for measurements in the high x and moderate Q^2 region. For example, at $x \approx 0.85$, the sensitivity of the deep inelastic structure function ratio $F_2^n(x, Q^2)/F_2^p(x, Q^2)$ to different deuteron wave functions corresponding to various realistic models of the nucleon-nucleon interaction is 20% [1]. Such large discrepancies make the accuracy of extracted neutron data inadequate for a thorough understanding of the dynamics of the nucleon's quark distribution.

To illustrate, consider the inclusive resonance electroproduction cross section spectra shown in Figure 1. These data were obtained at Jefferson Lab at $Q^2 = 1.5$ (GeV/c)^2 for hydrogen and deuterium at matched kinematics. While the three prominent resonance enhancements are obvious in the hydrogen data, only a hint of the first (the $\Delta(1232)$) is identifiable in the deuterium data. At $Q^2 > 2$ (GeV/c)^2, it is no longer possible to discern any structure in the deuterium data. Neutron extraction from this deuterium data will involve modelling the resonant and non-resonant components (as is pictured for the proton in the hydrogen data) for the neutron. Additionally, calculations will have to be made to account for the nuclear effects of binding, Fermi motion, and nucleon off-shellness. For each of these steps, a model-dependence will be introduced, the sum of which will lead to an overall substantial uncertainty in the knowledge of neutron resonance structure. It is for this reason that there exists very little neutron resonance transition form factor data.

Figure 2 depicts the existing $Q^2 > 1$ (GeV/c)^2 separated resonant and non-resonant contributions to the neutron to proton cross section ratio for the $\Delta(1232)$ resonance as a function of Q^2 [2]. There exist no other high Q^2 neutron resonance electroproduction data. The curve is from references [3, 4].

An average over Q^2 yields 0.72 ± 0.07 [2, 5] for the ratio, while an average over low Q^2 data yields $\sigma_n/\sigma_p = 0.91 \pm 0.03$ [6] for the Δ. It is interesting to note that the neutron Δ possibly exhibits the anomalous behavior seen in the proton data [7, 8, 9, 10]. Furthermore, in Figure 2(b), the non-resonant contribution is higher than that expected from deep inelastic results, which will be discussed below. Additionally, recent work [11] investigating Bloom-Gilman duality [12, 13] in the Δ resonance region suggests that there may be common dynamics between the resonance and the underlying nonresonant background, possibly hinting at interference effects.

It was found that the largest uncertainty in extracting the neutron data depicted in Figure 2 was the dependence of the assumed value of the neutron to proton cross section ratio for the S_{11} resonance, which is as yet unmeasured. A relativistic constituent quark model prediction for the $S_{11}(1535)$ resonance is approximately constant for $Q^2 > 1.5$ $(\text{GeV/c})^2$ at $\sigma_n/\sigma_p = 0.3$ [14].

Just as measurements of elastic and transition form factors provide information on the structure of the nucleon, measurements of the inelastic structure functions at large Q^2 reveal the quark structure of the nucleon. A large body of data exist on the ratio of the neutron to proton structure functions $F_2^n(x, Q^2)/F_2^p(x, Q^2)$ in deep inelastic scattering [15, 16, 17, 18, 3, 19, 20, 21]. The structure functions may be defined as follows:

$$\nu W_2(\nu, Q^2) \rightarrow F_2(x) = \Sigma_i e_i^2 x f_i(x) \tag{1}$$

and

$$M W_1(\nu, Q^2) \rightarrow F_1(x) = \frac{1}{2x} F_2(x). \tag{2}$$

The nucleons are made of partons with charges e_i^2. The parton momentum distribution $f_i(x)$ describes the probability that the struck parton i carries a fraction x of the nucleon's momentum. Rewriting the above equations in terms of the probability distributions of specific quark flavors, and neglecting the possibility of a sizeable presence of charm and heavier quarks inside the proton, yields:

$$\frac{1}{x}F_2^p = \frac{1}{9}[4u_V + d_V] + \frac{4}{3}S(x) \tag{3}$$

and

$$\frac{1}{x}F_2^n = \frac{1}{9}[u_V + 4d_V] + \frac{4}{3}S(x). \tag{4}$$

Here, $4/3$ is the sum of e_i^2 over the six sea quark distributions. At low x ($x \to 0$), the valence quarks are overshadowed by the multitudinous low momentum quark-antiquark pairs that make up the sea $S(x)$. When probing the large momentum part of the structure ($x \approx 1$), the fast valence quarks leave little momentum unoccupied for sea pairs. In this limit,

$$\frac{F_2^n(x)}{F_2^p(x)} \to \frac{u_V + 4d_V}{4u_V + d_V}. \tag{5}$$

Exact SU(6) spin-flavor symmetry in deep inelastic scattering would be manifested in equivalent shapes for the valence quark distributions, i.e. $u_V(x) = 2d_V(x)$ for all x, yielding

$$\frac{F_2^n(x)}{F_2^p(x)} \to \frac{2}{3}. \tag{6}$$

A well-documented deviation (see Figure 3 [22, 23]) from this result was seen in the deep inelastic data, which tends to $F_2^n/F_2^p \to 1/4$ at high x, indicating $u_V >> d_V$. In nature, SU(6) symmetry is broken; the nucleon and delta resonance masses are split by about 300 MeV. The symmetry breaking has been argued to arise from diquark configurations [24, 25]. A dominant scalar valence diquark component of the proton suggests that, in the $x \to 1$ limit, F_2^p is essentially given by a single quark distribution (the u_V) consistent with the F_2^n/F_2^p data.

However, reanalysis of existing data [1] using recent developments in the treatment of Fermi motion, binding, and nucleon off-shell effects in the

deuteron, suggests that the ratio may not be tending to 1/4 and may be more consistent with the perturbative QCD prediction that the ratio tend to the value 3/7 at large x. The 3/7 limit was formulated by Farrar and Jackson [26] in an approach where the total diquark spin projection is zero, i.e. as $x \to 1, S_z = 0$ for the spectators. In this case, the scattering may be from either a u or d quark, but scattering from a quark polarized in the opposite direction to the proton polarization is suppressed relative to the case where the interacting quark has the same spin orientation as the proton. A similar result has been obtained recently from a quark counting rule approach [27].

A summary of the predicted values for the ratio of the neutron to proton cross section in deep inelastic scattering may be found in Close [28]. The value of 1/4 is built into currently used phenomenological fits of the parton distribution [29, 30]. However, if one is to understand the dynamics of the nucleon's quark distributions at large x, it is imperative that the predictions outlined above be tested against experiment.

While much laudable effort has gone into accurate extraction of neutron information using deuterium targets, both experimentally and theoretically (see, for example, [31, 32, 33, 34] in addition to references already cited), large ambiguities still exist. Some current efforts use polarization degrees of freedom to assist with this difficulty. We propose to detect recoil protons in coincidence with scattered electrons from a deuteron target, thus creating a "tagged" neutron target. While there are many physics issues which can be addressed with the construction of this facility (elastic form factors, the EMC effect, test of spectator scaling, the Gottfried sum rule), we propose to focus initially on the neutron resonance region which can be easily accessed kinematically at Jefferson Lab and for which there is essentially no data available. Note that detecting the recoil proton and the scattered electron (and thus the q vector) also provides information on the R_{LT} interference structure function, due to the large out of plane acceptance. We also propose a preliminary measurement of the ratio F_2^n/F_2^p in the deep inelastic regime at $x = 0.65$ and $Q^2 = 5$ (GeV/c)^2. A conclusive measurement at $x = 0.8$ and $Q^2 = 5$ (GeV/c)^2 could be obtained with 9 GeV.

EXPERIMENTAL TECHNIQUE

We intend to tag electron-neutron scattering events by measuring the recoiling protons from a deuterium target in coincidence with the scattered electrons. Recent efforts indicate that this technique should be an effective tool for investigating neutron structure functions [35, 36]. An energy loss calculation shows that 140 (220) MeV/c protons reach a so-called neutron tag detector if originating in the center of a 1 cm (2.65 inch) diameter LD2 cryogenic target. This calculation takes the Al cell wall thickness (5 mil) and superinsulation layers into account, and assumes the proton has a vertex angle of $90 \pm 30°$. In practice this energy loss calculation and the detector response can well be calibrated using elastic e-p scattering. Here the elastically scattered electron tags a recoiling proton of well-defined energy, which energy can be monitored in the neutron tag detector.

To enable measurement of low-momentum recoiling protons we intend to build a 1 cm diameter cryogenic hydrogen/deuterium target. With such a target we can select protons with initial recoiling momenta between 150 and 200 MeV/c. Such a low recoiling momentum enhances greatly the possibility to estimate reliably the small off-shell effects related to the struck neutron. The fraction of recoiling protons between these momentum limits amounts to about 6%. For comparison, if we would use a standard Hall C cryogenic target (with a diameter of 2.65 inch), we would necessarily have to detect recoiling protons with vertex momenta larger than 220 MeV/c. This would reduce the fraction of detectable recoiling protons to $\approx$2%. Furthermore, the uncertainties in how to treat off-shell effects would grow undesirably large [37]. A 1 cm diameter cryotarget would still be large enough to allow for a $\pm$ 1 mm beam rastering, while the edges of the target are still $>>\pm 5\sigma$ away from the nominal beam position, to minimize large effects due to beam halo (a measurement in Hall C shows that the beam intensity is reduced with over 5 orders of magnitude at a distance of 5σ, while typical values for the beam size are $\sigma = 50 - 200\mu m$). We may construct a smaller diameter version of the 2.65 inch Hall C target cells for this experiment, or use a single-loop flowing cell. The performance of this target cell will, similar as with other target cells Halls C and A have used, be verified with a target boiling test, where count rates are monitored as a function of the current deposited on the target.

BACKGROUND RATES

Improvements in rate capability of vertex detectors over the last decades, particularly pushed by the high-energy physics community, enables this new neutron tagging technique. Previously, measurement of low-energy recoiling protons (or nuclei) was prohibited since it required a low-energy proton detector in close vicinity to a nuclear target, and thereby susceptible to all low-energy background associated with electron-nucleus interactions (either induced in the nuclear target or by the beam halo hitting external materials). Therefore, a high-rate capability is essential for a low-energy proton (neutron tag) detector.

Since most of the electron-associated background is in the forward hemisphere, we have chosen to put our detector at backward angles. Angles close to $90°$ in the laboratory system have been chosen to minimize the background rate and to minimize the energy loss of the recoiling protons in the cylinder-shaped cryogenic target cell. To illustrate the former point, we show in Figure 4 an example from the EMIN facility at NIKHEF, where the angular distribution of the instantaneous singles rate of an unshielded scintillator is depicted [38]. As one can see the count rate at angles above $80°$ is fairly flat, while the count rate below $70°$ is steeply rising.

We have performed two sets of background measurements in Hall C to measure both the general background rate and the low-energy proton singles rate associated with a 4 GeV electron beam hitting the Hall C LD2 target. Here we would like to add that the low-energy proton singles rates can not be calculated reliably with existing cross section parameterizations (EPC, Wiser's parameterization), since the use of these would indicate a typical 0.1-1 MHz/msr low-energy proton rate for electron-deuteron experiments, and would prohibit the use of unshielded scintillators at backward angles in an electron-accelerator facility. Empirically, such a huge rate of low-energy protons is not observed.

The first set of background measurements was performed in the spring of 1997, using a three-scintillator setup outside the Hall C scattering chamber (having a 16 mil Al vacuum window). The data were taken with a 40 μA, 4.0 GeV electron beam impinging on a 12 cm LD2 target. The coincidence

rate of the first two scintillators, with relatively high discriminator threshold settings to select highly-ionizing low-energy protons, was a few 100 Hz. The second set of background measurements, performed November 1997, used a two Si surface barrier detector setup inside the Hall C scattering chamber vacuum. The data were taken with an 80 μA, 4.0 GeV electron beam incident on a 4 cm LD2 target. Coincidence rates (with thresholds set by scope to catch the particles depositing large energies) were 1 kHz. In both cases the detectors were positioned such that they covered a 1 msr solid angle. We believe the 1 kHz/msr rate is a reasonable estimate for the low-momentum recoiling proton rate in the region of interest (between 100 and 200 MeV/c). Some of the very low momentum protons may not have escaped the 2.65 inch diameter standard Hall C LD2 cryotarget, but on the other hand some of the higher momentum protons, and possibly some deuterons, also deposit large amounts of energy in the detector layers, which we did not discriminate.

The singles rates in the first-layer detector was in all cases very high, typically a MHz. A comparison with Figure 4, the background rate measured at NIKHEF, scaled to an 80 μA electron beam current and a 640 mg/cm^2 LD2 target, amounts to 1.5 MHz/msr. Although the NIKHEF measurements were performed at a beam energy of 467 MeV, while we performed our simple tests at a beam energy of 4.045 GeV, and beam tune can obviously affect the rates, it seems reasonable to assume a worst-case scenario of a few MHz per msr background rate. A possible neutron tag detector therefore should be designed with these specifications in mind.

DETECTION SYSTEM

A sketch of the neutron tag detector is provided in Figure 5. We intend to build 6 scintillating fiber detectors of 20 × 12 cm, with 500 μm pitch, or, in the case of silicon strip, 10 × 6 cm, with 250 μm pitch. The detectors will be positioned at a distance of 20 cm (or 10 cm) from the beam axis, each covering a 30° section in out-of-plane angle ϕ and about a 40° section in scattering angle θ. Three detectors will be positioned at each side of the target, such that a total 90° section in out-of-plane angle is covered at each side.

Each detector will consist of two layers to perform ΔE-E type particle identification. As an example of this technique, we show in Figure 6 the results of a similar recoil detector operated at the NIKHEF AmPS ring [39]. This detector consists of two layers of silicon strip, of 100 and 475 μm thicknesses. The intrinsic time resolution of this system was 1.1 ns, the energy resolution a few 100 keV. Note that flight time corrections for these low-momentum protons can be big, therefore it helps to have both X and Y coordinates specified by the silicon strip layers. Recoiling protons with a vertex momentum of 150-200 MeV/c will reach the neutron tag detector with momenta of $100 - 200$ MeV/c, or kinetic energies of 5-20 MeV. Assuming a silicon strip detector with layers of 200 and 2000 μm thickness (250μm pitch) and a 1 cm diameter cryogenic LD2 cell (with 5 mil Al target thickness), protons with kinetic energies up to slightly above 20 MeV will stop in the second layer. Similarly, such protons will stop in the second layer of a scintillating fiber detector with layers of 500 and 5000 μm (500 μm pitch). Therefore, proton detection for protons in the momentum region of interest is well doable with either type of two-layer detector.

The effective solid angle of the suggested neutron tag detector amounts to $4\pi/9$ sr. Each channel of the detector covers an effective area of about 0.5 msr. Most of the background rate is expected to consist of γ's and low-energy electrons. Therefore especially the first layer will witness a high rate. The background test previously described indicated a background rate of a MHz per msr, for a luminosity of 10^{38} e-atoms/cm^2. The segmentation we have chosen will produce two channels for each msr, halving this background rate. Assuming a scintillating fiber detector, a few MHz per channel background rate is acceptable. Note that in various experiments at NIKHEF the large non-magnetic Hadron Detector devices were operated with rates of 3 MHz per scintillator paddle in the first detector layer.

Our background test also indicated a reduction of a factor of 10-100 in count rate of the second surface barrier detector with respect to the first surface barrier detector. Similarly, results in the AmPS storage ring at NIKHEF indicated a reduced rate with a factor of 100 in the second silicon strip layer, with respect to the first silicon strip detector of their recoil detector [39]. Trigger rates can easily be reduced by increasing the threshold settings for the electronics readout of the detectors, since the low-energy protons of interest deposit large energies in the detector layers.

A good timing resolution is of importance for these experiments to increase the real to accidental rates. If we assume that only 0.1% (worst case scenario) of the recoiling protons belonging to events where the neutron was struck by the high-energy electrons are detected, the real to accidental ratio is directly proportional to the proton singles rate (see previous section). For a luminosity of 10^{38} e-atoms/cm^2, corresponding to an 80 μA beam current impinging on a 4 cm LD2 target, the proton singles rate in the region of interest is expected to be about 1 kHz/msr. The full detector covers an area of about 1 sr, rendering a 1 MHz proton singles rate. Therefore, the real to accidental rate for a 1 ns resolving time is in this example about 1:1. Note that higher segmentation does not affect this real to accidental rate, but is only required to handle large non-proton background rates. By constructing a 1 cm diameter cryogenic LD2 target cell, we have boosted the measured fraction of recoiling protons to about 0.5%, thus improving the real to accidental ratio. We emphasize that this calculation assumes that none of the 1 kHz/msr protons we measured during the background tests actually belonged to recoiling protons of the e-n scattering process.

Recently, extensive work has been done at CERN on the development of scintillating fiber detectors using position sensitive photomultipliers. With 0.5 mm diameter fibers, a spatial resolution of 125μm and a timing resolution of 600 ps was obtained by the FAROS collaboration [40]. This research is particularly oriented towards the development of a topological trigger device. These characteristics are very close to our requirements.

EXPERIMENT

We propose to use the highest beam energy available at the time of the experiment. Table 1 lists the kinematics assuming a 6 GeV beam energy. We note that the count rates are not very sensitive to the exact beam energy, and the proposal could run with a beam energy of 5.5 GeV as well. We will use 4 cm long LD2 (and LH2) targets, and have assumed a beam current of 80 μA. We calculated the count rate estimates from e-p scattering data, taking into account that only 1 out of each 200 recoiling protons ends up

Table 1: 6 GeV Kinematics

HMS					
W^2	Q^2	E′	Θ	rate	time
$(\text{GeV/c})^2$	$(\text{GeV/c})^2$	GeV/c	deg	Hz	hours
1.54	1.02	5.10	10.5	240	0.5
2.89	0.89	4.45		190	0.5
4.04	0.78	3.90		120	0.5
1.52	1.42	4.95	12.5	85	0.5
2.81	1.25	4.35		88	0.5
4.00	1.09	3.80		67	0.5
1.47	1.94	4.70	15	19	1.5
2.84	1.69	4.10		30	1
3.99	1.48	3.60		26	1
1.51	2.46	4.40	17.5	5	6
2.85	2.15	3.85		11	3
4.06	1.87	3.35		11	3
1.54	2.99	4.10	20	1.7	16
2.84	2.62	3.60		4	6
4.01	2.30	3.15		5	6
1.46	3.54	3.85	22.5	0.6	48
2.85	3.08	3.35		2.0	16
3.97	2.71	2.95		2.5	12
TOTAL					122.5
SOS					
4.05	5.27	1.50	45	0.035	122.5
TOTAL					122.5

12

in the $4\pi/9$ sr detector (assuming recoiling protons with 150-200 MeV/c vertex momentum reach the detector), and that the neutron cross sections are lower than the proton cross sections. The HMS spectrometer will scan the resonance region to accumulate neutron resonance spectra, in the Q^2 range between 1.0 and 4.0 (GeV/c)^2. The SOS spectrometer with its large ($\pm 20\%$) momentum acceptance will be used to measure the $W^2 \approx 4$ region at relatively large x and Q^2 to compare the deep-inelastic neutron cross section to the deep-inelastic proton cross sections.

In all HMS spectra we estimate to accumulate 100K statistics, which corresponds to a 2% statistical uncertainty for a W^2 bin of 0.05 (GeV/c)^2. In the SOS spectrum we expect to accumulate 15K statistics. Current Hall C experiments indicate an additional 3% systematic uncertainty in total cross section measurements.

No additional data acquisition time for positron rate determinations is required. The chosen kinematics are all at a forward scattering angle, where previous SLAC and JLab measurements have indicated sub-1% positron contributions. We do require additional time for spectrometer momentum changes. We have assumed a 30 minute overhead for each spectrometer momentum change, which is larger than the 10 minute stabilization time typically used for Hall C experiments in 1996. Angle changes will be simultaneous with momentum changes. This amounts to an overhead of 9 hours. Therefore the total data acquisition time is 132 hours.

SUMMARY

We request a total time of 132 hours (5.5 days) to measure high-precision neutron resonance cross sections using a LD2 target. We request an additional day for installation of the detector in the Hall C scattering chamber, and an additional 3.5 day to checkout the detector, and calibrate both the detector (with elastic LH2 running) and the small-diameter cryotarget (boiling test). The total beam time request for this first-phase experiment amounts to 10 days, and is summarized in Table 2.

Table 2: Beam time request

Data acquisition (LD2)	122.5
18 momentum changes	9
Detector Calibrations (LH2)	24
Target boiling test	12
Detector Installation	24
Detector Checkout	48
Total	**240**

References

[1] W. Melnitchouk and A.W. Thomas, Phys. Lett. B377 (1989) 11.

[2] L. Stuart et al, SLAC-PUB-6305 (1996), submitted to Phys. Rev. D.

[3] L.W. Whitlow et al., Phys. Lett. 282B (1992) 475.

[4] P. Amaudruz et al, Phys. Lett. 295B (1992) 159.

[5] S. Rock et al, Phys. Rev. D46 (1992) 24.

[6] M. Kobberling et al, Nucl. Phys. B82 (1974) 201.

[7] P. Stoler, Phys. Reports 226, 103 (1993).

[8] P. Stoler, Phys. Rev. Lett. 66, 1003 (1991).

[9] P. Stoler, Phys. Rev. D44, 73 (1991).

[10] C. Keppel, Proceedings of the Workshop on CEBAF at Higher Energies, eds. N. Isgur and P. Stoler (April 1994) 237

[11] C. Carlson and N. Mukhopadhyay, Phys. Rev. D47 (1993) R1737.

[12] E.D. Bloom and F.J. Gilman, Phys. Rev. Lett. 25 (1970) 1140.

[13] E.D. Bloom and F.J. Gilman, Phys. Rev. D4 (1971) 2901.

[14] M. Warns et al, Phys. Rev. D42 (1990) 2215

[15] J.J. Aubert et al., Nucl. Phys. B293 (1987) 740.

[16] A.C. Benvenuti et al., Phys. Lett. 237B (1990) 599.

[17] P. Amaudruz et al., Nucl. Phys. B371 (1992) 3.

[18] A. Bodek and J.L. Ritchie, Phys. Rev. D23 (1981) 1070.

[19] M Arneodo et al, Phys. Lett. 364B (1995) 107.

[20] M Arneodo et al, Nucl. Phys. B483 (1997) 3.

[21] M Arneodo et al, Nucl. Phys. B487 (1997) 3.

[22] E. Bloom, Proceedings of the 6th International Symposium on Electron and Photon Interactions, Bonn (1973)

[23] A. Bodek et al, Phys. Lett. 51B (1974) 417.

[24] F.E. Close, Phys. Lett. 43B (1973) 422.

[25] R. Carlitz, Phys. Lett. 58B (1975) 345.

[26] G.R. Farrar and D.R. Jackson, Phys. Rev. Lett. 35 (1975) 1416.

[27] S.J. Brodsky, M. Burkardt, and I. Schmidt, Nucl. Phys. B441 (1995) 197.

[28] F. Close, An Introduction to Quarks and Partons, Harcourt Brace Jovanovich (1979) 304

[29] CTEQ Collaboration, H.L. Lai et al, Phys. Rev. D51 (1995) 4763

[30] A.D. Martin, R. Roberts, and W.J. Stirling, Phys. Rev. D50 (1994) 6734

[31] W. Melnitchouk A.W. Schreiber, and A.W. Thomas, Phys. Lett. B335 (1994) 11.

[32] M.A. Braun and M.V. Tokarev, Phys. Lett. 320B (1994) 381.

[33] A. Lung et al, Phys. Rev. Lett. 70 (1993) 718.

[34] L.P. Kaptari and A. Yu. Umnikov, Phys. Lett. B 259 (1991) 155

[35] S. Simula, Phys. Lett. B 387 (1996) 245

[36] S. Simula, Proceedings of the FBXV Conference in Groningen (1997)

[37] W. Melnitchouk, M. Sargsian, M. Strikman, Proceedings of the '95-'96 Workshop on Future Physica at HERA, Future Physics with Light and Heavy Nuclie at HERMES, ed. G. van der Steenhoven (1996) p.53

[38] A. Zondervan, Ph.D. Thesis, University of Amsterdam (1992)

[39] M. van Sambeek, Ph.D. Thesis, Free University of Amsterdam (1997)

[40] V. Agoritsas et al, CERN-PPE-96-143 (1996), submitted to Nucl. Inst. Methods
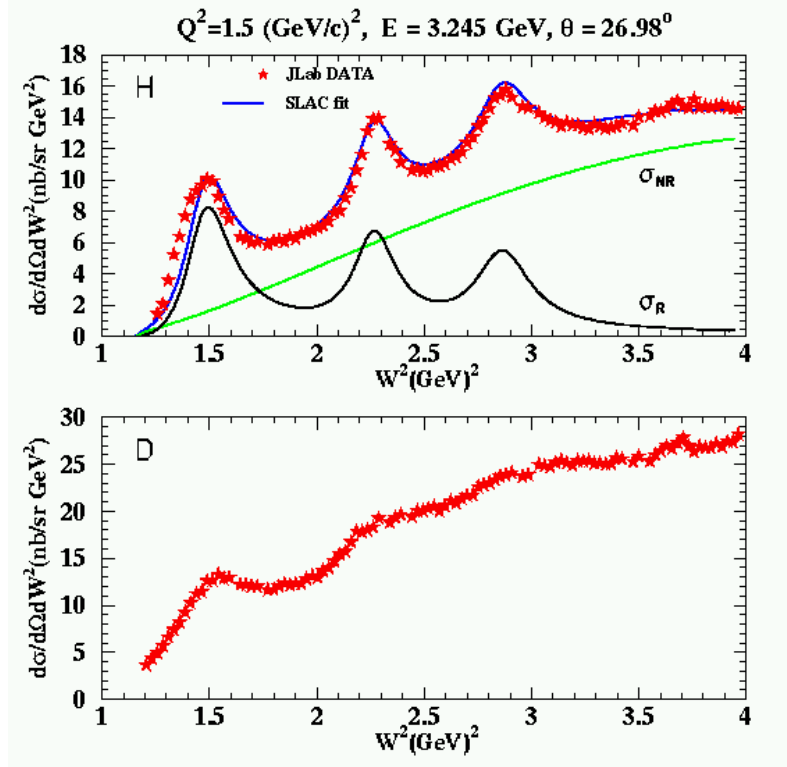
Figure 1: Inclusive resonance electroproduction cross sections from Jefferson Lab at $Q^2 = 1.5$ $(\mathrm{GeV/c})^2$. Cross sections are shown as a function of invariant mass squared. The top spectrum is from a hydrogen target and the bottom is from deuterium at matched kinematics. The hydrogen spectra are plotted with total global fit results as well as the resonant and non-resonant fit components.
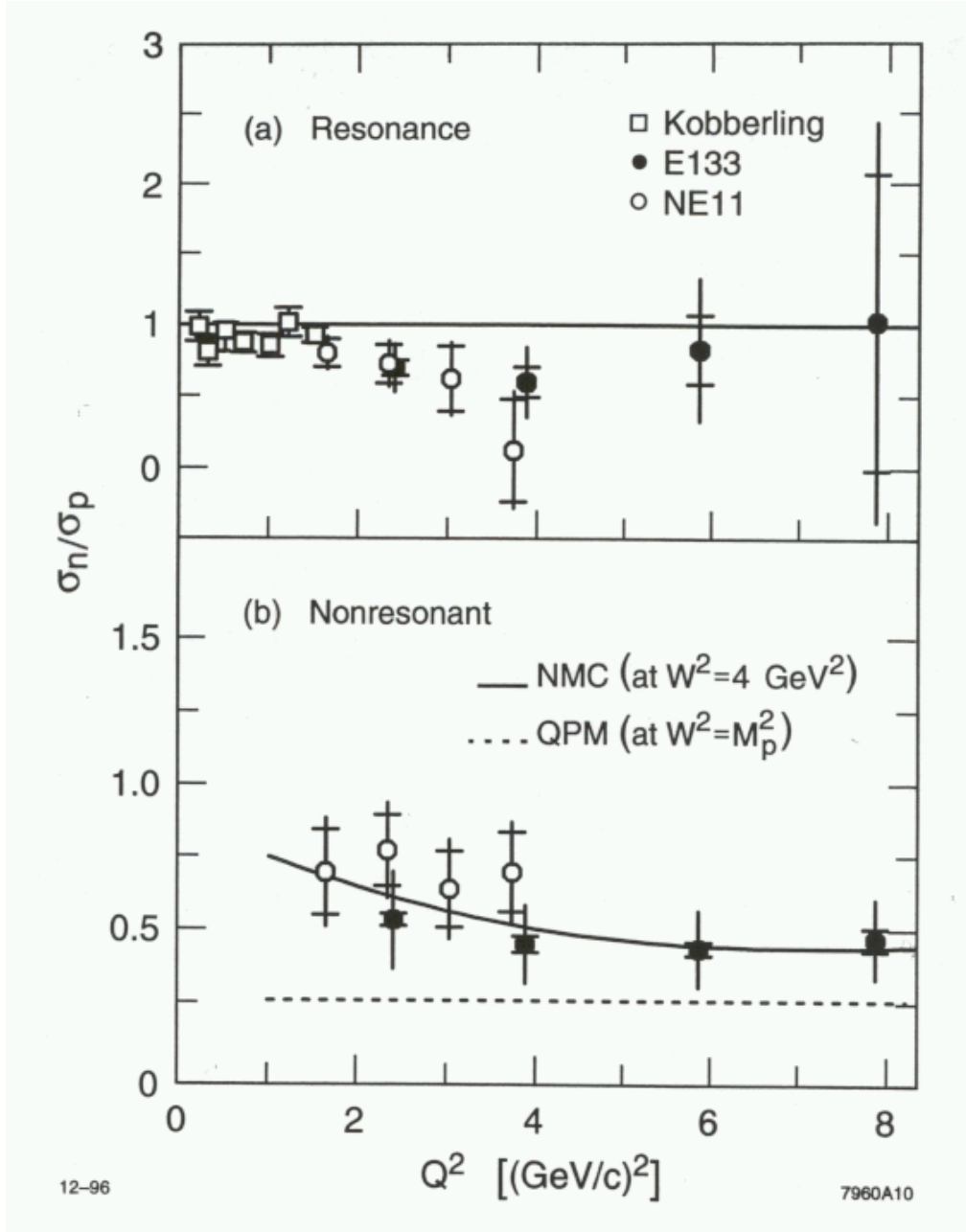
Figure 2: Ratios (a) σ_n/σ_p for the delta resonance and (b) for the nonresonant background extracted from fit. The inner error bar is statistical and the outer error bar is systematic including modelling uncertainties.
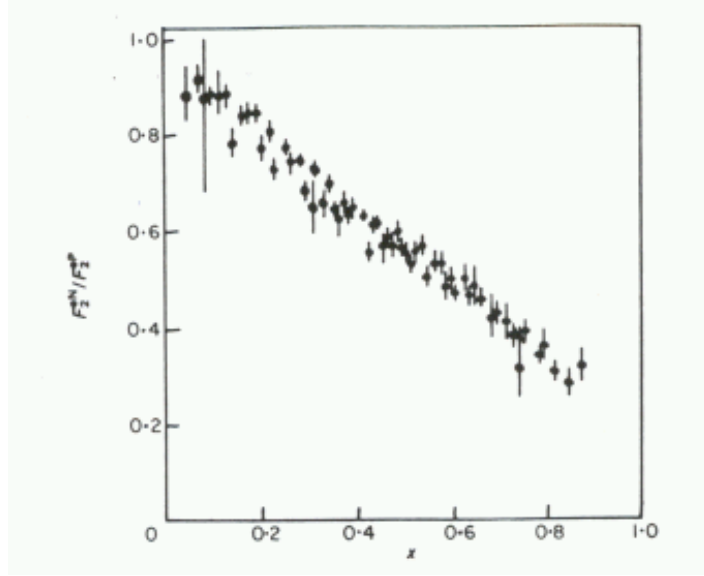
18

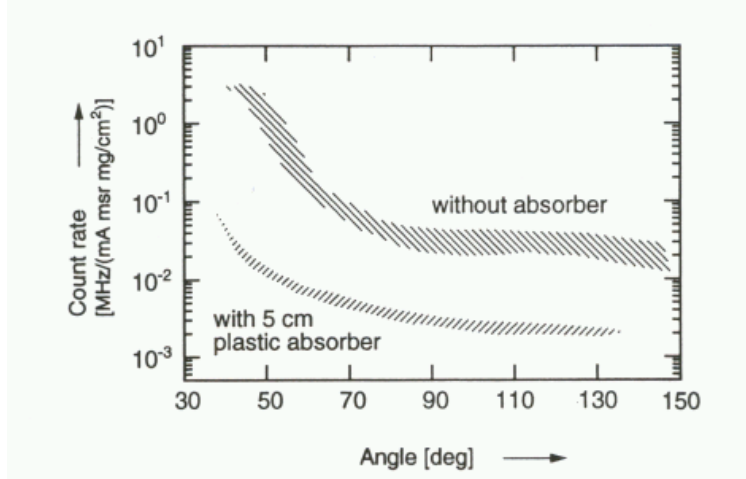Figure 3: The ratio F_2^n/F_2^p as a function of x for deep inelastic electron scattering.

Figure 4: Angular distribution of the instantaneous singles count rate of a 0.5 cm thick scintillator with no absorber, and a 5 cm thick scintillator with 5 cm of plastic in front of it. The threshold setting is just above the noise and the error band illustrates the sensitivity of the count rate with respect to the precision of this definition.
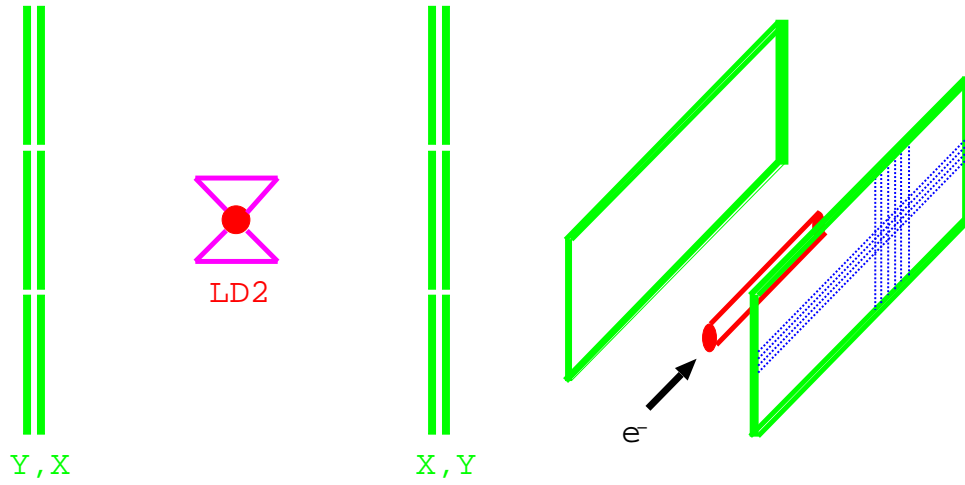
Figure 5: A sketch of the neutron tagging detector. The detectors will be positioned at a distance of 20 cm from the beam axis, and will cover a 90° section in out-of-plane angle and a 40° section in scattering angle θ. Each detector will consist of two layers to perform ΔE-E particle identification.
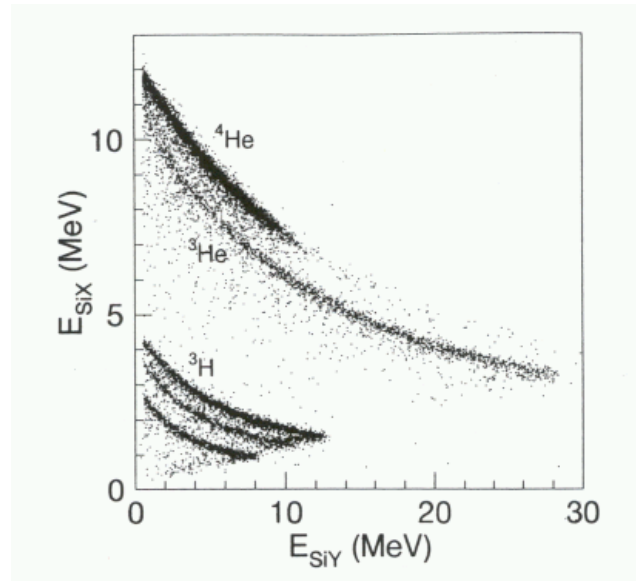

Figure 6: Energy loss in 100 μm silicon strip horizontal (SiX) detector versus loss in 475 μm silicon strip vertical (SiY) detector, for a fraction of the data obtained at the NIKHEF AmPS ring. The particles were stopped in the SiY detector and the bands corresponding to different particles are clearly visible.